Abstract

Carbon dioxide (CO_2) efflux from soil represents one of the biggest ecosystem carbon (C) fluxes and high-magnitude pulses caused by rainfall make a substantial contribution to the overall C emissions. It is widely accepted that the drier the soil, the larger the CO_2 pulses will be, but this notion has never been tested for water-repellent soils. Soil water repellency (SWR) is a common feature of many soils and is especially prominent after dry periods or fires. An important unanswered question is to what degree SWR affects common assumptions about soil CO_2 dynamics. To address this, our study investigates, for the first time, the effect of SWR on the CO_2 pulse upon wetting for water-repellent soils from recently burned forest sites. CO_2 efflux measurements in response to simulated wetting were conducted both under laboratory and *in situ* conditions. Experiments were conducted on strongly and extremely water-repellent soils, with a wettable scenario simulated by adding a wetting agent to the water. CO_2 efflux upon rewetting was significantly lower in the water-repellent scenarios. Under laboratory conditions, CO_2 pulse was up to four times lower under the water-repellent scenario as a result of limited wetting, with 70% of applied water draining rapidly via preferential flow paths, leaving much of the soil dry. We suggest that the predominant cause of the lower CO_2 pulse in water-repellent soils was the smaller volume of pores in which the CO_2 was replaced by infiltrating water, compared to wettable soil. This study shows that SWR should be considered as an important factor when measuring or predicting the CO_2 flush upon rewetting of dry soils. Although this study focused mainly on short-term effects of rewetting on CO_2 fluxes, the overall implications of SWR on physical changes in soil conditions can be long lasting, with overall larger consequences for C dynamics.

Keywords: hydrophobicity, Birch effect, wildfire, wetting, rain pulses, pore degasification, climate change

Highlights:

- CO_2 pulse upon wetting was markedly lower under water-repellent conditions.
- 70 % of water applied to water-repellent soils quickly drained out of the samples.
- Most pores in water-repellent soils were not filled with water upon wetting.
- Low refilling of air-filled pores upon wetting resulted in a low CO_2 pulse.

1. Introduction

Carbon dioxide (CO_2) emissions from soils represent the largest terrestrial carbon (C) flux to the atmosphere (Longdoz et al., 2000). Given that soil moisture is one of the main controllers of the soil C efflux (Davidson and Janssens, 2006; Moyano et al., 2013), there is great concern that alteration of precipitation patterns due to climate change could result in a reduction of soil C storage and an increase in emissions (Falloon et al., 2011). Drought periods followed by heavy rainfall events have already become more frequent and extreme in many regions (Coumou and Rahmstorf, 2012; Trenberth et al., 2014). Extended dry periods result in severe reduction of soil moisture vital to sustain many aspects of soil functioning (IPCC, 2018). Lack of available water in soil pores reduces microbial activity and root respiration rates (Moyano et al., 2013; Or et al., 2007), resulting in overall low soil CO_2 efflux to the atmosphere.

Rewetting of dry soils has been associated with a sudden, large pulse of CO_2 to the atmosphere known as the 'Birch effect' (Birch, 1958), recognised as a key contributor to soil C losses and representing a large fraction of the overall C flux (Leon et al., 2014; Smith et al., 2017). This CO_2 pulse is believed to originate predominantly from a rapid restoration of microbial respiration caused by microbial biomass growth (Waring and Powers, 2016) and activation of extracellular enzymes (Fraser et al., 2016; Smith et al., 2017) as water availability increases pore connectivity

50 and mobilizes previously unavailable C (Kim et al., 2012; Marañón-Jiménez et al., 2011; Schimel,
51 2018). Part of the rewetting CO_2 pulse is assigned to degassing of air-filled pores as CO_2 is often
52 stored in the available pore-space and not always released instantly (Maier et al., 2011). Several
53 factors influence the size of this wetting pulse. Low soil moisture prior to wetting as a result of
54 longer and more intense drying periods has been linked to an increase in the size of the CO_2 pulse
55 (Meisner et al., 2017), while the rewetting of soil at optimum moisture levels results in smaller
56 pulses (Muhr and Borken, 2009). The size of the CO_2 pulse is expected to increase with larger
57 wetting intensities, i.e., rate and amount of water added (Lado-Monserrat et al., 2014; Muhr and
58 Borken, 2009; Sponseller, 2007) as well as with lower frequencies of the drying-wetting cycles
59 (Christensen and Prieme, 2001; Fierer and Schimel, 2002). Several reviews have specifically
60 focused on the Birch effect, addressing the effects of drying and rewetting on CO_2 fluxes and C
61 mineralization (Jarvis et al., 2007; Muhr and Borken, 2009), rewetting effects on CO_2 fluxes (Kim
62 et al., 2012) and modelling the CO_2 efflux from responses to moisture changes (Moyano et al.,
63 2013; Vicca et al., 2014).

64 A few studies have reported unexpectedly low CO_2 fluxes upon rewetting of very dry soil,
65 speculating that the lack of CO_2 flush upon rewetting could be due to soil water repellency (SWR)
66 (Lado-Monserrat et al., 2014; Muhr and Borken, 2009) reducing water infiltration into the soil.
67 This explanation may seem reasonable given that SWR is a common feature of dry soil under
68 permanent vegetation and many drought-affected soils undergo temporal physical
69 transformation to prevent further moisture loss, which does not readily revert with addition of
70 water (Schimel, 2018). However, none of the aforementioned studies suggesting that the lack of
71 CO_2 flush upon rewetting is due to SWR actually performed any SWR measurements, so this
72 explanation remains speculative. Therefore, a clear research gap exists regarding the effect of
73 SWR on CO_2 efflux upon rewetting, especially given that future climate scenarios, predicting
74 greater drought and more wildfires, are likely to enhance the development of SWR (Goebel et al.,
75 2011; Muhr and Borken, 2009).

Very little is known about the effect of SWR on CO_2 efflux and how inhibited infiltration will affect the release of CO_2 to the atmosphere. In a field-based study in the UK, Urbanek and Doerr (2017) focused specifically on the effect of water repellency on CO_2 effluxes. They observed lower CO_2 effluxes under severe and uniformly distributed SWR than under patchy SWR and moisture distribution. Soil respiration in water-repellent soils has also been addressed under laboratory conditions (Goebel et al., 2007; Goebel et al., 2005), but the few prior studies focused on overall CO_2 emission rates, rather than CO_2 emissions rates occurring during rewetting events. Furthermore, relatively little is known about the effect of the first rainfall on CO_2 emissions from fire-affected soils. Fire is known to enhance SWR at or below the soil surface (Mataix-Solera et al., 2011; Moody et al., 2013; Shakesby and Doerr, 2006) simultaneously it has a direct effect on carbon pools (Amiro et al., 2003; Bond-Lamberty et al., 2007; Meigs et al., 2009) and reduces microbial activity due to sterilization (Mataix-Solera et al., 2009). The first post-fire rainfall event will play a major role in activating the recovery of soil respiration. Similar to unburnt soil, the wetting of recently burned soil has been shown to induce a short-lived CO_2 pulse (Castaldi et al., 2010; Marañón-Jiménez et al., 2011; Pinto et al., 2002; Vargas et al., 2012), which is possibly enhanced by the input of nutrients from scorched plant material and/or ash (Concilio et al., 2006; Marañón-Jiménez et al., 2011).

Although water repellency is a common feature of fire-affected soils (Shakesby and Doerr, 2006), there is a clear lack of understanding of how SWR may affect soil CO_2 effluxes from burnt soils. Areas affected by recent fire are likely to exhibit water repellency and combined with their lack of surface vegetation during the initial post-fire period, provide ideal conditions for isolating the effects of SWR on the Birch effect. Therefore, the aim of our study was to test the hypothesis that SWR suppresses CO_2 effluxes upon wetting of burnt soils. The objectives were to: I) compare the CO_2 response to wetting under wettable and water-repellent scenarios at the core (cm) scale under controlled laboratory conditions; II) examine the CO_2 responses to wetting in relation to

SWR and changes in soil moisture and III) validate the CO_2 response to wetting under field conditions.

2. Research design and methods

This study comprises a series of wetting experiments and CO_2 efflux measurements on water-repellent soils in fire-affected areas: *i*) under laboratory conditions on intact core soil samples and *ii*) *in situ* under field conditions. Soil sampling and *in situ* measurements were carried out at two sites within a recently burned forest in October 2017, two months after a wildfire and before the first major rainfall in the area. Fire severity at the study site was classified by the European Forest Fire Information System (EFFIS, 2017) as moderate to high. Field observations during the first month after the fire revealed that consumption of the tree crowns as well as of the litter layer were generally complete, and that the ash layer was predominantly black. Both sites are located in Central Portugal in Vale das Casas, 7 km South East of the municipality of Vila de Rei and were affected by the same wildfire event in August 2017. A field survey and soil profile description revealed that the predominant soil type of the study site was an arenic skeletic Regosol (FAO, 2014), derived from sedimentary sandstone. The climate in the area is classified as hot-summer Mediterranean, with annual precipitation of 900 mm y^{-1}, average air temperature of 14 °C (with maximum and minimum air temperatures of 42 °C and -1 °C, respectively) and wind direction predominantly NW. To be able to assess the hydrological effect of differing topographies on the CO_2 pulse after wetting, site 1 is located in a burnt pine forest *(Pinus pinaster)* on flat terrain, while site 2 is located in a pine-dominated (*Pinus pinaster*) forest with some eucalyptus (*E. globulus*) on a slope (approx. 30°, facing ESE) (Table 1). At site 1, the ~2 cm layer of black ash was retained untouched with only the pine needles removed from the surface; hence this site is called burnt with ash (BwA). At site 2, both the pine needles and the layer of back ash (~2 cm thick) were brushed off the surface, exposing the bare soil to simulate the removal of the ash layer by

wind erosion. Including a bare soil (BnoA) in the experimental design helps to understand the influence of an ash layer on wetting and CO_2 efflux. Air temperature during sampling and field measurements ranged between 23 and 31°C with the exception of the 15th October, which coincided with measurements in the BwA site plot 4, when temperatures reached up to 37°C.

Individual intact cores and field plots were subjected to one of two rewetting treatments: water only, to observe the response of water-repellent soils, and water mixed with a wetting agent (Revolution®, Aquatrols, 1:42) to alleviate water repellency, thus simulating wettable soil. Preliminary tests confirmed that the addition of the wetting agent itself did not affect microbial activity in the soil (Lewis, 2019). All samples were rewetted from above to simulate a rainfall event. In the laboratory, effluxes were monitored from above and below the soil sample in order to capture movement of CO_2 in both directions.

2.1 Laboratory methods

Intact cores (8 cm diameter, 5 cm height) were collected from both study sites near the *in situ* measurement plots. Fifteen soil cores were collected from each site along a 12 m transect (3 cores × 5 sampling points) from 0 - 5 cm depth in metal cylinders. Pine needles were removed from the surface before sampling in the BwA site, leaving the ash layer (~2 cm) on the surface. Pine needles together with the ash layer were removed from the surface in the BnoA site, exposing the mineral soil before sampling (Fig. 1). After sampling, plastic caps were immediately fitted to the cylinders to preserve soil moisture which were then thereafter stored at 4 °C. Prior to the wetting experiments, the samples were equilibrated at 20 °C for 24 h.

The cores were rewetted from above using a custom-made rainfall simulator fitted between the soil collar and the CO_2 flux chamber. The rainfall simulator comprised one spiral tube with uniformly distributed drips, to ensure spatially uniform wetting, suspended 1 cm above the soil surface and connected via a tube to a large syringe to supply water. All cores received one single

and uniform wetting event of 25 mm with an intensity of 100 mm h^{-1}. The amount of water applied to soil cores was equivalent to 80 % of water-filled pore-space (WFPS) and the duration of wetting was approximately 15 min. WFPS was calculated individually for each core by dividing volumetric water content by pore space. Pore space (PS) was obtained from soil bulk density (dB) as follows: $PS = (1 - dB\ d_p^{-1}) \times 100$; assuming a particle density (d_p) = 2.65 g cm^{-3} (Blake, 2008). Water retention was measured as the weight difference in the soil before and after wetting. Percolation time was determined, and drained water was collected and quantified.

Each core was suspended on a set of collars allowing monitoring of the CO_2 concentration in the chamber above and below the sample during the rainfall simulation, and collection of the drained water (supplementary Fig. 1). The CO_2 concentration was monitored via a 10 cm survey chamber connected to an infrared CO_2 analyser system (IRGA, Li-8100A) from above (Li-COR Inc.) and a plastic container with a similar headspace connected to a separate IRGA CO_2 analyser system below the sample. A fine mesh was placed under the cores to allow any drainage of water while holding the core inside the cylinder. The entire system (chambers, rainfall simulator and soil sample) was sealed to avoid gas leakage. The chamber's inbuilt pressure vent helped maintain ambient pressure inside the chamber (supplementary Fig. 1). CO_2 effluxes were monitored in 30 min intervals with 1 min for pre and post-purge, over a total of 340 min. Initial CO_2 effluxes were measured before wetting, during the simulated rainfall, which lasted approximately 15 min, and for 270 min after the rainfall.

Of the three intact cores obtained at each sampling point, two were randomly allocated to one of the rewetting treatments. The third core was used to determine soil water content (SWC) and SWR distribution at different depths prior to wetting, following the subsampling method of Liu et al. (2019) which involved sampling the core in 5 locations at 5 different depths using a small ring of 1 cm height by 2 cm diameter (supplementary Fig. 2). A custom-made Plexiglas disk (1 cm height, 7.9 cm diameter) was placed under the soil core to bring the soil upwards. After

176 subsampling, the remaining soil was removed from the surface with a knife. This process was
177 repeated for each cm of the 5 cm depth of the soil cores.

178 SWR prior to wetting was determined for each of the core's subsamples following the water drop
179 penetration test (WDPT) (Doerr, 1998) by applying 3 drops of water to the surface of each
180 subsample and measuring the infiltration time of each drop. 15 drops in total were applied to
181 each layer of the core (3 drops × 5 subsampling points per layer). Drops were applied using a
182 pipette to equalise drop size. Infiltration times were categorised into the following classes (Doerr,
183 1998): wettable (< 5 s), slightly repellent (5-60 s), moderately repellent (60-600 s), strongly
184 repellent (600-3600) and extremely repellent (> 3600 s).

185 SWC of the subsamples was determined by calculating the weight loss of the sample after drying
186 at 105 °C for 24 h (van Reeuwijk, 2002). The five oven-dried subsamples per layer were combined
187 into one sample per layer to determine soil organic matter (loss of ignition, Nelson and Sommers
188 (1996)) and particle size distribution (laser diffraction, Beckman Coulter, Inc.). The remaining
189 sample was pooled into a single sample and hand sieved through a 25 mm mesh size to
190 determine stone content (Urbanek & Shakesby, 2009).

191

192 ## 2.2 Field methods

193 At each study site, four 1 m^2 plots were selected along a 12 m transect. At each plot four PVC
194 collars (12 cm height, 20 cm diameter) were installed, two for measuring soil CO_2 efflux and two
195 others for measuring SWC and soil temperature. Although not ideal, it was necessary to install
196 SWC and temperature sensors in separate collars than those designated for CO_2 monitoring to
197 avoid soil disturbance and potential changes to the CO_2 efflux response. Two SWC and
198 temperature sensors (ECH_2O 5-TM, Meter-Group, USA) were installed horizontally, opposite to
199 each other at 3 cm below the surface of the mineral soil (supplementary Fig. 3) and monitored
200 continuously for the duration of the observations. PVC collars were inserted into the soil at least

24 h before the beginning of the experiments, approximately 8 cm into the soil, leaving an offset of 3 to 4 cm to place the CO_2 analyser chamber and provide a strong seal.

The rainfall simulations were performed using a watering can with the distributor applying one single and uniform rainfall event of 25 mm at an intensity of 100 mm h^{-1} during 15 min to simulate a heavy rainfall event. CO_2 efflux was measured using a Li-8100A infrared gas analyser system with a 20 cm survey chamber (LI-COR, Inc.) before, immediately after wetting and at 15, 30, 60, 90 and 120 minutes after the end of wetting. At each observation time, three 2 min measurements were taken.

2.3 Data analysis

The CO_2 concentration data obtained was fitted exponentially excluding the first 30 s of measurements, which is the typical time required to achieve steady mixing inside the chamber (LICOR, 2010). The following equation (Eq.1) was applied to calculate CO_2 efflux as the rate of change in CO_2 concentration released from soil (LICOR, 2010):

Eq.1
$$Fc = \frac{10VPo\left(1-\frac{Wo}{1000}\right)}{RS(To+273.15)} * \frac{dC'}{dT}$$

Fc = soil CO_2 efflux (µmol m^{-2} s^{-1}), V = volume (cm^3), Po = initial pressure (kPa), Wo =initial water vapour mole fraction (mmol mol^{-1}), S = soil surface area (cm^2), To = initial air temperature (°C) and dC'/dT = initial rate of change in water-corrected CO_2 mole fraction (µmol mol^{-1}). CO_2 efflux data below $R^2 \geq 0.95$ were rejected with a total of 1.3 % of total rejected measurements. CO_2 flux graphs were created by calculating the mean flux for each treatment at each measurement time, along with 95% confidence intervals and standard deviation for laboratory and field graphs respectively. The estimated CO_2 flux pulses under field conditions were calculated proportionally to the size of the pulse observed under laboratory conditions for the same soil and wetting

scenario. The Mann-Whitney U-test was applied to test for statistical differences between wetting scenarios. Statistical differences were accepted at $p < 0.05$.

Spatial frequency graphs of SWR were obtained by calculating the percentage of WDPT measurement points per soil depth falling into each WDPT category (Doerr, 1998). The Kolmogorov-Smirnov two-sample test was applied to determine statistically significant differences ($p < 0.05$) in water repellency between the five different depths analysed. A linear regression analysis was performed between cumulative flux and the change in SWC with wetting in all soils under field and laboratory conditions.

3. Results

3.1 CO_2 efflux prior to and after wetting

3.1.1 Laboratory measurements

CO_2 efflux prior to wetting was very low in all soils under laboratory conditions ranging between 0 and 1 µmol m^{-2} s^{-1} (Fig. 2). CO_2 effluxes increased immediately in response to the simulated rainfall. The CO_2 pulse under water-repellent conditions (orange line in Fig. 2) was significantly lower in both soils ($p = 0.024$, $p = 0.005$ in the BwA and BnoA respectively) compared to wettable conditions, but the duration of the peak was relatively similar. The effluxes decreased rapidly with the end of wetting and stabilized at approximately 10 to 15 min after wetting, remaining at a constant value until the end of the observation (4.5 h after wetting). The CO_2 effluxes were slightly above pre-wetting values by the end of the observation period, but <1 µmol m^{-2} s^{-1} in all cases. The CO_2 efflux observed below the sample was very close to the pre-wetting values and no significant CO_2 response to the wetting event was observed.

The mean size of the CO_2 pulse, under water-repellent conditions, was <1.5 µmol m^{-2} s^{-1}, whereas peaks nearly 4 times higher were observed under wettable conditions (4.4 and 5 µmol m^{-2} s^{-1} in

248 the BnoA and BwA soil respectively). Similarly, the cumulative efflux from soil under water-
249 repellent conditions was half (9 and 10 µmol m^{-2} s^{-1} in the BnoA and BwA) of that measured under
250 wettable conditions (20 and 22 µmol m^{-2} s^{-1} in the BnoA and BwA; p = 0.005, p = 0.024
251 respectively) (Fig. 3). The overall cumulative CO_2 efflux upon wetting was proportional to the
252 change in SWC, as shown in Fig. 4.

253

254 *3.1.2 Field measurements*

255 Under field conditions, the CO_2 efflux prior to wetting was low, ranging from 0.98 to 2.1 µmol m^{-2}
256 s^{-1} in the BwA and BnoA soil respectively. An increase in the CO_2 efflux was observed in response
257 to wetting, but the CO_2 efflux decreased steadily after the wetting stopped. At both sites and for
258 both water-repellent and wettable scenarios, the CO_2 efflux remained above pre-wetting values
259 by the end of the observations (120 min after the start of wetting) and no significant differences
260 were observed between wetting scenarios at the end of the observations.

261 The observed CO_2 efflux peak was especially high in the BwA plots, reaching values of 12 µmol m^{-2}
262 s^{-1} for the water-repellent scenario and 17 µmol m^{-2} s^{-1} for the wettable scenario. The CO_2 efflux
263 in response to wetting observed in the BnoA soil was lower than in the BwA soil, reaching values
264 of 5 and 4 µmol m^{-2} s^{-1} under wettable and water-repellent scenarios respectively. The duration
265 of the pulse was shorter in the BnoA soil, lasting only up to 30 min after the start of wetting (Fig.
266 5).

267 Field *in situ* experiments allowed CO_2 efflux measurements only after the rainfall simulations. The
268 estimated CO_2 pulse reached lower values under water-repellent (12 and 6 µmol m^{-2} s^{-1} in the BwA
269 and BnoA respectively) than under wettable conditions (29 and 10 in the BwA and BnoA
270 respectively).

The size of the CO_2 pulse, calculated as the difference between the peak efflux and the average efflux prior to wetting, was higher, although not significantly, under wettable (5 and 16 µmol m^{-2} s^{-1} in the BnoA and BwA site respectively) compared to water-repellent conditions (4 and 12 µmol m^{-2} s^{-1} in the BnoA and BwA site respectively) ($p = 0.074$, $p = 0.124$ in the BwA and BnoA, respectively, between wettable and water-repellent conditions) (Fig. 3). Overall, the field-scale cumulative efflux (Fig. 3), which included the height and the duration of the peak, was lower, but not significantly, under water-repellent conditions, with average values ranging between 107 and 71 µmol m^{-2} s^{-1} in the BwA and BnoA respectively ($p = 0.074$, $p = 0.282$); while the cumulative efflux under wettable conditions oscillated between 126 and 75 µmol m^{-2} s^{-1} in the BwA and BnoA respectively.

3.2 Water repellency distribution prior to wetting

All soils exhibited SWR prior to wetting, but its distribution varied strongly with soil depth and the presence of ash (Fig. 6). At the surface layer (0 - 1 cm depth) in the BwA soil, 64 % of measured points, directly on the ash layer, were water-repellent (WDPT > 5 s); while for BnoA, water repellency was significantly higher than in the BwA soil ($p < 0.001$) with 100 % of sample points classified as water-repellent of which 80 % were in the extreme SWR class (WDPT > 3600 s) (Fig. 6).

In the BwA soil, similar SWR distribution to the surface layer was observed in the 1 - 2 cm depth layer (62 % of points water-repellent), but further down, at 2 - 3 cm depth, SWR increased significantly ($p = 0.01$) with up to 88 % of points classified as water-repellent. The percentage of SWR decreased with depth, reaching 60 % of points classified as water-repellent at the 4 - 5 cm depth. It is worth noting that although the overall percentage of water-repellent soil was the highest at 2-3 cm depth, the percentage of soil in the extreme water-repellent class was the highest (47 %) at 4 - 5 cm depth in comparison with the lowest percentage (19 %) at 1 - 2 cm

296 depth. Slightly different patterns of SWR distribution with depth were observed in the BnoA soil,
297 where the percentage of SWR decreased steadily and significantly with depth (from 95 % at 1 - 2
298 cm to 45 % at 4 - 5 cm depth; $p < 0.001$ in all cases), with a proportional decrease in the
299 percentage of extreme water-repellent points (from 50 % at 1 – 2 cm to 28 % at 4 - 5 cm depth).

300 An exception was found between 3 - 4 and 4 -5 cm depth were the difference in SWR distribution
301 was not significant ($p = 0.68$).

302

303 ## 3.3 Soil moisture prior to and after wetting

304 ### *3.3.1 Laboratory measurements*

305 Prior to wetting, all soils under wettable and water-repellent conditions (0 - 5 cm) were very dry,
306 with mean SWC (vol.) values below 2 % and 4 % for BwA and BnoA respectively (Table 2). Upon
307 wetting, SWC increased by 16 % and 8 % for BwA and BnoA soils respectively in the water-
308 repellent scenario, while in the wettable scenario, the observed SWC change was significantly
309 higher ($p < 0.001$) increasing by 47 % in BwA soil and 33 % in BnoA soil (Table 2). In this laboratory
310 set up, water was able to drain out of the soil samples, resulting in 76 and 82 % (BwA and BnoA
311 respectively) drainage in the water-repellent scenario, starting within 3 minutes of the start of
312 wetting. Drainage was significantly lower under wettable conditions with only 14 % and 36 %
313 (BwA and BnoA, respectively) beginning at approximately 9 min after the start of wetting (Table
314 3).

315 SWC within the intact cores before wetting was low and rather uniformly distributed, falling
316 within the 0 - 10 % SWC class. Wetting resulted in a significant increase in SWC at all soil depths
317 under both water-repellent and wettable scenarios ($p < 0.001$) (6), except at 2 - 3 cm depth in the
318 BnoA soil. The difference in SWC after wetting was especially pronounced in the BwA soil, where
319 surface SWC (0 - 1 cm depth) under water-repellent conditions was nearly half that under
320 wettable conditions for the same depth (Fig. 7 A and B). The difference in SWC in the BwA site is

more pronounced with depth, with SWC approximately 3 times lower under water-repellent conditions. The distribution of SWC after wetting was highly variable (Fig. 8) and larger variation was observed under water-repellent conditions (coefficient of variation, CV = SD Mean^{-1}, ranging from 67 to 84 % and 39 and 73 % in the BwA and BnoA soil respectively).

3.3.2 Field measurements

The wetting experiments in the field resulted in infiltration into all soils under both water-repellent and wettable scenarios, with an increase in SWC observed in all plots. However, depending on the wetting treatment, the change in SWC was very variable. SWC in the soil wetted with water increased significantly by 14 and 16% in the BwA and BnoA with respect to pre-wetting values ($p < 0.001$). The soil wetted with the wetting agent reached significantly higher SWC values ($p = 0.035$) than in the water-repellent scenario, resulting in a significant increase in SWC of 17 % and 23 % in BwA and BnoA with respect to pre-wetting values ($p < 0.001$) (Table 2). Infiltration differed between the sites. In the BwA, on flat terrain, 100 % infiltration was observed in both collars, those wetted with water and those with water and a wetting agent. While at the BnoA site, situated on a 30° slope, 100 % infiltration was also observed under wettable conditions whilst under water-repellent conditions, 65 % of the total water added infiltrated into the soil with the remaining 35 % transformed into overland flow and leaving the respiration collar without infiltrating.

4 Discussion

The first significant wetting after the fire, simulated in the experiment, resulted in a distinct CO_2 pulse under both field and laboratory conditions, but the magnitude of the peak strongly depended on the type of wetting scenario and the presence of ash on the soil surface.

345 The CO_2 pulse was observed during and immediately after wetting under the wettable scenario,
346 whereas wetting of water-repellent soils showed significantly lower peaks, especially in the
347 laboratory experiment (Fig. 3). Under water-repellent conditions, the applied water initially
348 ponded on the surface due to extreme water repellency inhibiting uniform infiltration, but then
349 percolated quickly through the sample, within 3 min after the start of wetting, with up to 70 % of
350 applied water draining out of the soil (Table 3). Such behaviour is very typical for water-repellent
351 soil and has been commonly observed by others under field (e.g. Leighton-Boyce et al., 2007) or
352 laboratory conditions (e.g. Urbanek and Shakesby, 2009; Urbanek et al., 2015) in fire-affected as
353 well as unburnt water-repellent soils. This quick percolation resulted in a limited replacement of
354 air in air-filled pores by water in the soil matrix and hence a low CO_2 pulse. The very low SWC in
355 many areas of the soil samples after wetting (Fig. 7 and 8) supports this interpretation. We expect
356 that movement of water via preferential flow paths resulted in a fractured distribution of SWC,
357 and areas of water-filled pores were adjacent to areas of air-filled pores. It is likely that
358 preferential infiltration increased the pore pressure along the wetting path and facilitated gas
359 movement to air-filled pores of lower pore pressure. These aeration channels within the soil
360 matrix would facilitate gas exchange between the soil matrix and the atmosphere. Smith et al.
361 (2017) argued that hydraulic connectivity at the pore-scale is an important factor affecting CO_2
362 dynamics after wetting, based on the observation that cumulative CO_2 efflux was higher when
363 larger pores where connected first, during a rainfall event, as opposed to smaller pores filling
364 first, for example, during capillary rise wetting.

365 Under a wettable scenario, the even increase in SWC throughout the samples suggests that the
366 wetting front moved relatively evenly downwards, refilling most soil pores with water, resulting in
367 the much higher CO_2 pulse observed (Fig. 4).

368 The wetting experiment under field conditions confirmed the observations from the laboratory.
369 The CO_2 pulses were much higher here, but the differences between the wettable and water-

370 repellent scenarios were slightly less distinct. Furthermore, the differences between the CO_2
371 pulses from soil in flat terrain with the ash remaining (BwA) and the site on the slope with the ash
372 removed (BnoA) were very significant.

373 The observed overall larger CO_2 fluxes in the field experiment would be expected because of the
374 larger pore volume of the whole soil profile in comparison to the shorter soil sample cores used in
375 the laboratory. Other studies observed similar (Castaldi et al., 2010; Marañón-Jiménez et al.,
376 2011; Vargas et al., 2012), or even higher (Marañón-Jiménez et al., 2011) CO_2 peaks from field
377 rainfall simulations, presumably because of the deeper soil profiles, compared to the shallow soils
378 present at our study sites.

379 The actual CO_2 pulses in the field were likely to have been even higher than what we measured as
380 it was not possible to measure the CO_2 flux during the wetting and hence measurements started
381 only after the addition of water was completed. Indeed, the laboratory experiments showed the
382 largest peak to occur during the wetting, suggesting that the actual peak in the field experiment
383 might have been twice as high (as shown in the Fig. 5). We expect that this large peak during the
384 rewetting is also often not captured in other field studies because of limitations in the frequency
385 of measurements when using automated soil CO_2 flux monitoring systems or due to other
386 methodological challenges during rainfall events when measuring with the long-term eddy
387 covariance techniques.

388 In the field wetting experiment, very distinct differences in CO_2 flux responses were observed
389 between the study sites. BwA exhibited much higher CO_2 peaks with a distinct difference between
390 wetting scenarios, while BnoA had much lower CO_2 peaks and no significant differences between
391 wettable and water repellent scenarios.

392 We expect that the presence of ash contributed to the magnitude of the pulse for a range of
393 reasons. The ash layer remaining on the surface was able to absorb and retain substantially more
394 water (Table 2) than the mineral soil underneath. A higher volume of refilled pores would have

resulted in larger CO_2 pulses. The presence of an ash layer also affected the SWR distribution (Fig. 6) and consequently the infiltration and the water distribution pattern (Fig. 7 and 8). In BwA, the first 2 cm of the soil only 60 % of points exhibited water repellency as opposed to the top mineral layer, which showed up to 100 % of water-repellent points (Fig. 6). Water-repellent ash has been observed after low severity fires and is mainly related to the organic C content of the samples but, in most cases, wildfire ash has been observed to be wettable (see review by Bodí et al., 2014). Depending on its initial wettability, the incorporation of ash into the soil matrix can enhance or reduce SWR (Bodí et al., 2011). Such patchy distribution of SWR suggests that water infiltration was irregular, possibly even favouring a rapid gas exchange between the soil and the atmosphere. Urbanek and Doerr (2017), who investigated the effect of water repellency on CO_2 efflux, suggested that patchy SWR can provide very favourable conditions for soil respiration and gas diffusion, because water-repellent zones can create aeration channels adjacent to infiltration paths, in which gas exchange is stimulated.

Another potentially important contribution to the CO_2 pulse might result from abiotic processes such as the chemical reaction of carbonates with wetting. Calcium carbonate produced from the burning of organic matter at high temperatures is commonly observed in wildfire ash (Bodí et al., 2014; Dlapa et al., 2013; Pereira et al., 2012). Carbonates are known to contribute substantially to CO_2 fluxes in calcareous soils (Bertrand et al., 2007; Serrano-Ortiz et al., 2010) or to the rapid flush of CO_2 with wetting observed during the incubation of biochar in soil (Bruun et al., 2014). However, in this case, the addition of acid to the ash suggested low to no presence of carbonates. We therefore expect that the contribution to CO_2 flux from carbonates in the ash layer was negligible. Further studies would be beneficial to understand the role of ash on CO_2 emissions from soil, with a special focus on the specific contribution of ash to CO_2 fluxes after the fire.

It was surprising to find very low CO_2 pulses after wetting of soils at BnoA, and much lower ($p = 0.172$) differences between the wettable and water-repellent scenarios. We expect that the

420 removal of ash was the main reason for the low CO_2 pulses, but we anticipate that the slope of
421 the study site also contributed to it. Increased overland flow is commonly recognized in post-fire
422 environments on slopes where SWR inhibits infiltration, sometimes causing mass movement of
423 the remaining ash down the slopes (Bodí et al., 2012). It was observed (although not shown in the
424 results) that simulated wetting directly on completely water-repellent mineral soil resulted in
425 overland flow, but this was partially blocked by the soil collar and caused ponding of water at the
426 lower part of the collar. We expect some concentrated infiltration occurred at the lower part of
427 the collar resulting in the infiltration and the main gas exchange occurring outside of the collar,
428 which was not captured in the measuring chamber.

429 The duration of the peak we have observed is relatively short, but it is in line with other studies
430 (Marañón-Jiménez et al., 2011; Munson et al., 2010; Rey et al., 2017; Sponseller, 2007; Wang et
431 al., 2016). For example, Rey et al. (2017), during a field study observed CO_2 effluxes peaking only
432 15 minutes after wetting during *in situ* rain manipulation experiments. The short duration of the
433 peak could suggest that the flush of CO_2 is mainly caused by degassing (Inglima et al., 2009; Liu et
434 al., 2002), with water refilling the air-filled pores and displacing the CO_2-rich air previously stored
435 in the pore space (Maier et al., 2011; Schymanski et al. 2017). Although the input of sudden
436 increase in microbial respiration cannot be fully excluded, we suspect that it had a rather low
437 contribution to this initial CO_2 pulse, as fire suppresses microbial activity due to sterilization
438 (Mataix-Solera et al., 2009), along with low microbial respiration caused by lack of available water
439 (Göransson et al., 2013). We expect that the wetting patterns caused by water repellency will
440 have long lasting implications on the overall recovery of soil respiration, an area that warrants
441 attention in future studies.

442 Although this study focused mainly on the short-term and immediate effects of rewetting of post-
443 burn soils on CO_2 efflux, we anticipate that the overall impact of fire on physical changes to soil
444 conditions are rather long lasting. Fire is known to change the overall C flux system from a sink to

445 a source of CO_2 (Irvine et al., 2007). These so-called 'hot moments', with sudden short-lived but
446 high-magnitude spikes in C release from soil, can have a cumulative effect after rainfall events
447 and make up a substantial fraction of the annual C balance (Leon et al., 2014; Smith et al., 2017).
448 In our study, the CO_2 peak accounted for 78% of the total CO_2 released during the observation in
449 both BwA and BnoA soil under wettable conditions. Schymanski et al. (2017) reported a CO_2 flush
450 of similar magnitude when rewetting a sterilised soil, as a result of physical replacement of CO_2 by
451 water, as when rewetting natural soils under field conditions. In a longer observation, Castaldi et
452 al. (2013) quantified that the pulse of CO_2 in burnt soils, which peaked during the first day after
453 water addition, accounted for about 50% of the total CO_2 emissions over a 15-day observation
454 period. Marañón-Jiménez et al. (2011) observed during an *in situ* rewetting study of recently
455 burned soil that up to 64% of the total CO_2 released during the first 2 hours after wetting was
456 related to degasification of CO_2-rich air in soil pores. Similarly, Maier et al. (2010) showed that
457 during extreme rainfall events, up to 20% of the total flux originated from CO_2 stored in the pore-
458 space prior to the wetting event. While the degassing effect with wetting is short-lived, on the
459 scale of minutes to hours after wetting, overlooking the release of previously stored CO_2 might
460 result in overestimations of the contribution of microbial mineralization to the Birch effect.

461 The longer-term effects of preferential infiltration on microbial respiration are still not fully
462 understood and future studies should aim at incorporating the dynamic alterations in soil
463 hydraulic functions as a result of SWR (Robinson et al., 2019). Most soils show some degree of
464 repellency, however, models are still limited in their ability to include spatial variability of water
465 content and, when calculating C fluxes, represent only average changes in soil moisture.

466 It is also important to keep in mind that SWR is not only a feature of burnt soils, extreme water
467 repellency is also commonly observed in dry, unburnt soils (Doerr et al., 2000). Under our
468 changing climate, a higher frequency and intensity of droughts followed by large rainfall events is
469 expected. Water repellency is, therefore, likely to become more common and severe (Goebel et

al., 2011). Although the current study was carried out on fire-affected soils, we anticipate that a similar CO_2 efflux behaviour of dry soils in response to rainfall can be expected in any soils affected by water repellency. How common and distinct this behaviour is, however, remains to be confirmed by further studies.

5. Conclusions

Our study, which focused on investigating the effect of water repellency on CO_2 efflux upon rewetting of recently burned soils, has confirmed that SWR does reduce the Birch effect. Both laboratory and field-based experiments showed that infiltration and percolation patterns in water-repellent soils were concentrated along preferential flow paths, resulting in substantial drainage of applied water and very low rewetting rates of the soil matrix. The smaller the overall changes were in SWC, the lower the cumulative efflux from the soil was, suggesting that concentrated flow in water-repellent soils results in smaller volumes of CO_2-filled pores replaced by water and a lower Birch effect. The study has also shown that the ash layer remaining on the surface of burnt soils contributed substantially to the overall CO_2 flush upon rewetting, most likely due to its higher absorption and retention rates than the mineral soil.

Although this study focused mainly on the short-term and immediate effect of rewetting of burnt soils on CO_2 efflux, which is predominantly caused by soil degassing, the overall implications of fire with regards to physical changes in soil conditions can be expected to be long lasting. Given that fire overturns the overall C flux system from a sink to a source of CO_2, the short-lived but high-magnitude spikes in C release from soil after rainfall are likely to make up a substantial fraction of the annual C balance. It is therefore important to consider SWR as an important factor affecting the rewetting patterns of soil and reducing the CO_2 efflux when calculating and predicting overall C fluxes between soil and the atmosphere. It is also important to remember that SWR is not only a feature of burnt soils but also that extreme water repellency is also

commonly observed in dry, unburnt soils. Therefore, we expect similar behaviour in any soil affected by water repellency.

Acknowledgements

CSG and EU were supported by the Royal Society – Research Fellows Enhancement Award 2017 (RGF\EA\180262) and Dorothy Hodgkin Fellowship (DH110189), both awarded to EU. SD was supported by NERC (grant NE/R011125/1) and OECD (contract TAD/CRP JA 95401). BO and JJK were supported by the project FIRE-C-BUDs (PTDC/AGR-FOR/4143/2014 - POCI-01-0145-FEDER-016780) funded by FEDER, through COMPETE2020 - Programa Operacional Competitividade e Internacionalização (POCI), and by national funds (OE), through FCT/MCTES, as well as by CESAM, through the strategic project UID/AMB/50017, funded by national funds (OE), through FCT/MCTES. JJK also acknowledges his FCT-IF contract (IF/01465/2015), through FCT/MCTES. We thank Aquatrols® for providing the wetting agent used in the experiments. We would also like to thank Óscar González-Pelayo for providing the soil classification of the study site and to Julia Kelly for careful proofreading of the manuscript. Furthermore, we are grateful to three anonymous reviewers and the editor for their constructive comments.

References

Amiro, B. D., Macpherson, J. I., Desjardins, R. L., Chen, J. M., Liu, J. (2003). Post-fire carbon dioxide fluxes in the western Canadian boreal forest: evidence from towers, aircrafts and remote sensing. *Agricultural and Forest Meteorology*, *115*, 91–107. https://doi.org/https://doi.org/10.1016/S0168-1923(02)00170-3

Bertrand, I., Delfosse, O., Mary, B. (2007). Carbon and nitrogen mineralization in acidic, limed and calcareous agricultural soils: apparent and actual effects. *Soil Biology and Biochemistry*, *39*,

276–288. https://doi.org/10.1016/j.soilbio.2006.07.016

Birch, H. F. (1958). The effect of soil drying on humus decomposition and nitrogen availability. *Plant and Soil*, *10*, 9–31. https://doi.org/10.1007/BF01343734

Bodí, M. B., Doerr, S. H., Cerdà, A., Mataix-Solera, J. (2012). Hydrological effects of a layer of vegetation ash on underlying wettable and water repellent soil. *Geoderma*, *191*, 14–23. https://doi.org/10.1016/j.geoderma.2012.01.006

Bodí, M. B., Martin, D. A., Balfour, V. N., Santín, C., Doerr, S. H., Pereira, P., Cerdà, A., Mataix-Solera, J. (2014). Wildland fire ash: production, composition and eco-hydro-geomorphic effects. *Earth Science Reviews*, *130*, 8252. https://doi.org/10.1016/j.earscirev.2014.07.005

Bodí, M. B., Mataix-Solera, J., Doerr, S. H., Cerdà, A. (2011). The wettability of ash from burned vegetation and its relationship to Mediterranean plant species type, burn severity and total organic carbon content. *Geoderma*, *160*, 599–607. https://doi.org/10.1016/j.geoderma.2010.11.009

Bond-Lamberty, B., Peckham, S. D., Ahl, D. E., Gower, S. T. (2007). Fire as the dominant driver of central Canadian boreal forest carbon balance. *Nature*, *450*, 89–92. https://doi.org/10.1038/nature06272

Bruun, S., Clauson-Kaas, S., Bobuľská, L., Thomsen, I. K. (2014). Carbon dioxide emissions from biochar in soil: role of clay, microorganisms and carbonates. *European Journal of Soil Science*, *65*, 52–59. https://doi.org/10.1111/ejss.12073

Castaldi, S., de Grandcourt, A., Rasile, A., Skiba, U., Valentini, R. (2010). CO_2, CH_4 and N_2O fluxes from soil of a burned grassland in Central Africa. *Biogeosciences*, *7*, 3459–3471. https://doi.org/10.5194/bg-7-3459-2010

Christensen, S., Prieme, A. (2001). Natural perturbations, drying-wetting and freezing-thawing cycles, and the emission of nitrous oxide, carbon dioxide and methane from farmed organic

544 soils. *Soil Biology*, *33*, 2083–2091. https://doi.org/10.1016/S0038-0717(01)00140-7

545 Concilio, A., Ma, S., Ryu, S., North, M., Chen, J. (2006). Soil respiration response to experimental
546 disturbances over 3 years. *Forest Ecology and Management*, *228*, 82–90.
547 https://doi.org/10.1016/j.foreco.2006.02.029

548 Coumou, D., Rahmstorf, S. (2012). A decade of weather extremes. *Nature Climate Change*, *2*, 491.
549 https://doi.org/https://doi.org/10.1038/nclimate1452

550 Davidson, E. A., Janssens, I. A. (2006). Temperature sensitivity of soil carbon decomposition and
551 feedbacks to climate change. *Nature*, *440*, 165–173. https://doi.org/10.1038/nature04514

552 Dlapa, P., Bodí, M. B., Mataix-Solera, J., Cerdà, A., Doerr, S. H. (2013). FT-IR spectroscopy reveals
553 that ash water repellency is highly dependent on ash chemical composition. *Catena*, *108*,
554 35–43. https://doi.org/10.1016/j.catena.2012.02.011

555 Doerr, S. H. (1998). On standardizing the 'Water Drop Penetration Time' and the 'Molarity of an
556 Ethanol Droplet' techniques to classify soil hydrophobicity: a case study using medium
557 textured soils. *Earth Surface Processes and Landforms*, *23*, 663–668.
558 https://doi.org/10.1002/(SICI)1096-9837(199807)23:7<663::AID-ESP909>3.0.CO;2-6

559 Doerr, S. H., Shakesby, R. A., Walsh, R. P. D. (2000). Soil water repellency: Its causes,
560 characteristics and hydro-geomorphological significance. *Earth Science Reviews*, *51*, 33–65.
561 https://doi.org/10.1016/S0012-8252(00)00011-8

562 EFFIS, 2017. COPERNICUS – Emergency Management Service.
563 https://effis.jrc.ec.europa.eu/static/effis_current_situation/public/index.html

564 Falloon, P., Jones, C. D., Ades, M., Paul, K. (2011). Direct soil moisture controls of future global soil
565 carbon changes: An important source of uncertainty. *Global Biogeochemical Cycles*, *25*.
566 https://doi.org/10.1029/2010GB003938

567 Fierer, N., Schimel, J. P. (2002). Effects of drying-rewetting frequency on soil carbon and nitrogen
568 transformations. *Soil Biology and Biochemistry*, *34*, 777–787.

569 Fraser, F. C., Corstanje, R., Deeks, L. K., Harris, J. A., Pawlett, M., Todman, L. C., Whitmore, A. P.,
570 Ritz, K. (2016). On the origin of carbon dioxide released from rewetted soils. *Soil Biology and*
571 *Biochemistry*, 101, 1-5. https://doi.org/10.1016/j.soilbio.2016.06.032

572 Goebel, M. O., Bachmann, J., Reichstein, M., Janssens, I. A., Guggenberger, G. (2011). Soil water
573 repellency and its implications for organic matter decomposition - is there a link to extreme
574 climatic events? *Global Change Biology*, *17*, 2640–2656. https://doi.org/10.1111/j.1365-
575 2486.2011.02414.x

576 Goebel, M. O., Bachmann, J., Woche, S. K., Fischer, W. R. (2005). Soil wettability, aggregate
577 stability, and the decomposition of soil organic matter. *Geoderma*, *128*, 80–93.
578 https://doi.org/10.1016/j.geoderma.2004.12.016

579 Goebel, M. O., Woche, S. K., Bachmann, J., Lamparter, A., Fischer, W. R. (2007). Significance of
580 wettability-induced changes in microscopic water distribution for soil organic matter
581 decomposition. *Soil Science Society of America Journal*, *71*, 1593–1599.
582 https://doi.org/doi:10.2136/sssaj2006.0192

583 Göransson, H., Godbold, D. L., Jones, D. L., Rousk, J. (2013). Bacterial growth and respiration
584 responses upon rewetting dry forest soils: Impact of drought-legacy. *Soil Biology and*
585 *Biochemistry*, *57*, 477–486. https://doi.org/10.1016/j.soilbio.2012.08.031

586 Inglima, I., Alberti, G., Bertolini, T., Vaccari, F. P., Gioli, B., Miglietta, F., Cotrufo, M. F., Peressotti,
587 A. (2009). Precipitation pulses enhance respiration of Mediterranean ecosystems: the
588 balance between organic and inorganic components of increased soil CO_2 efflux. *Global*
589 *Change Biology*, *15*, 1289–1301. https://doi.org/10.1111/j.1365-2486.2008.01793.x

590 Irvine, J., Law, B. E., Hibbard, K. A. (2007). Postfire carbon pools and fluxes in semiarid ponderosa

591 pine in Central Oregon. *Global Change Biology*, *13*, 1748–1760.
592 https://doi.org/10.1111/j.1365-2486.2007.01368.x

593 IUSS Working Group WRB. 2015. World Reference Base for Soil Resources 2014, update 2015
594 International soil classification system for naming soils and creating legends for soil maps.
595 World Soil Resources Reports No. 106. FAO, Rome.

596 Jarvis, P., Rey, A., Petsikos, C., Wingate, L., Rayment, M., Pereira, J., Banza, J., David, F., Miglietta,
597 F., Borghetti, M., Manca, F., Valentini, R. (2007). Drying and wetting of Mediterranean soils
598 stimulates decompositionand carbon dioxide emission: the "Birch effect." *Tree Physiology*,
599 *27*, 929–940. https://doi.org/10.1093/treephys/27.7.929

600 Kim, D. G., Vargas, R., Bond-Lamberty, B., Turetsky, M. R. (2012). Effects of soil rewetting and
601 thawing on soil gas fluxes: a review of current literature and suggestions for future research.
602 *Biogeosciences*, *9*, 2459–2483. https://doi.org/10.5194/bg-9-2459-2012

603 Lado-Monserrat, L., Lull, C., Bautista, I., Lidón, A., Herrera, R. (2014). Soil moisture increment as a
604 controlling variable of the "Birch effect". Interactions with the pre-wetting soil moisture and
605 litter addition. *Plant and Soil, 379*, 21–34. https://doi.org/10.1007/s11104-014-2037-5

606 Leighton-Boyce, G., Doerr, S. H., Shakesby, R. A., Walsh, R. P. D. (2007). Quantiying the impact of
607 soil water repellency on overland flow generation and erosion: a new approach using rainfall
608 simulation and wetting agent on in situ soil. *Hydrological Processes*, *21*, 2337–2345.
609 https://doi.org/10.1002/hyp.6744

610 Leon, E., Vargas, R., Bullock, S., Lopez, E., Rodrigo, A., La, N., Jr, S. (2014). Hot spots, hot moments,
611 and spatio-temporal controls on soil CO_2 efflux in a water-limited ecosystem. *Soil Biology*
612 *and Biochemistry*, *77*, 12–21. https://doi.org/10.1016/j.soilbio.2014.05.029

613 Lewis, C. R. (2019). *The effect of rewetting with surfactant (Aquatrols®) on soil microbial*
614 *communities*. Swansea University, BSc dissertation thesis.

615 Liu, Z., Rahav, M., Wallach, R. (2019). Spatial variation of soil water repellency in a commercial
616 orchard irrigated with treated wastewater. *Geoderma*, *333*, 214–224.
617 https://doi.org/10.1016/j.geoderma.2018.07.021

618 Longdoz, B., Yernaux, M., Aubinet, M. (2000). Soil CO_2 efflux measurements in mixed forest:
619 impact of chamber disturbance, spatial variability and seasonal evolution. *Global Change*
620 *Biology*, *6*, 907–917. https://doi.org/10.1046/j.1365-2486.2000.00369.x

621 Maier, M., Schack-Kirchner, H., Hildebrand, E. E., Holst, J. (2010). Pore-space CO_2 dynamics in a
622 deep, well-aerated soil. *European Journal of Soil Science*, *61*, 877–887.
623 https://doi.org/10.1111/j.1365-2389.2010.01287.x

624 Maier, M., Schack-Kirchner, H., Hildebrand, E. E., Schindler, D. (2011). Soil CO_2 efflux vs. soil
625 respiration: implications for flux models. *Agricultural and Forest Meteorology*, *151*, 1723–
626 1730. https://doi.org/10.1016/j.agrformet.2011.07.006

627 Marañón-Jiménez, S., Castro, J., Kowalski, A. S., Serrano-Ortiz, P., Reverter, B. R., Sánchez-Cañete,
628 E. P., Zamora, R. (2011). Post-fire soil respiration in relation to burnt wood management in a
629 Mediterranean mountain ecosystem. *Forest Ecology and Management*, *261*, 1436–1447.
630 https://doi.org/10.1016/j.foreco.2011.01.030

631 Masson-Demotte, V., Zhai, P., Pörtner, H. O., Roberts, D., Skea, J., Shukla, P. R., Pirani, A.,
632 Moufouma-Okia, C., Péan, C., Pidcok, R., Connors, S., Matthews, J. B. R., Chen, T., Zhou, X.,
633 Gomis, M. I., Lonnoy, E., Maycock, T., Tignor, M., Waterfield, T. (2018). *Global warming of 1.5*
634 *°C. An IPCC Special Report on the impacts of global warming of 1.5 °C above pre-industrial*
635 *levels and related global greenhouse gas emission pathways, in the context of strengthening*
636 *the global response to the threat of climate chang*e. Retrieved from
637 https://www.ipcc.ch/sr15/

638 Mataix-Solera, J., Cerdà, A., Arcenegui, V., Jordán, A., Zavala, L. M. (2011). Fire effects on soil

639 aggregation: A review, *Earth-Science Review, 109*, 44–60.
640 https://doi.org/10.1016/j.earscirev.2011.08.002

641 Mataix-Solera, J., Guerrero, C., Garcia-Orenes, F., Barcenas, G. M., Torres, M. P. (2009). Forest fire
642 effects on soil microbiology. In *Fire effects on soils and restoration strategies*.
643 https://doi.org/10.1201/9781439843338-c5

644 Meigs, G. W., Donato, D. C., Campbell, J. L., Jonathan, G., Law, B. E. (2009). Forest fire impacts on
645 carbon uptake, storage and emission: the role of burn severity in the Eastern Cascades,
646 Oregon. *Ecosystems*, *12*, 1246–1267. https://doi.org/10.1007/s10021-009-9285-x

647 Meisner, A., Leizeaga, A., Rousk, J., Bååth, E. (2017). Partial drying accelerates bacterial growth
648 recovery to rewetting. *Soil Biology and Biochemistry*, *112*, 269–276.
649 https://doi.org/10.1016/j.soilbio.2017.05.016

650 Moody, J. A., Shakesby, R. A., Robichaud, P. R., Cannon, S. H., Martin, D. A. (2013). Current
651 research issues related to post-wildfire runoff and erosion processes. *Earth Science Reviews*,
652 *122*, 10–37. https://doi.org/10.1016/j.earscirev.2013.03.004

653 Moyano, F. E., Manzoni, S., Chenu, C. (2013). Responses of soil heterotrophic respiration to
654 moisture availability: an exploration of processes and models. *Soil Biology and Biochemistry*,
655 *59*, 72–85. https://doi.org/10.1016/j.soilbio.2013.01.002

656 Muhr, J., Borken, W. (2009). Delayed recovery of soil respiration after wetting of dry soil further
657 reduces C losses from a Norway spruce forest soil. *Journal of Geophysical Research*, *114*,
658 G04023. https://doi.org/10.1029/2009JG000998

659 Munson, S. M., Benton, T. J., Lauenroth, W. K., Burke, I. C. (2010). Soil carbon flux following pulse
660 precipitation events in the shortgrass steppe. *Ecological Research*, *25*, 205–211.
661 https://doi.org/10.1007/s11284-009-0651-0

662 Or, D., Smets, B. F., Wraith, J. M., Dechesne, A., Friedman, S. P. (2007). Physical constraints

affecting bacterial habitats and activity in unsaturated porous media - a review. *Advances in Water Resources*, *30*, 1505–1527. https://doi.org/10.1016/j.advwatres.2006.05.025

Pereira, P., Úbeda, X., Martin, D. A. (2012). Fire severity effects on ash chemical composition and water-extractable elements. *Geoderma*, *191*, 105–114. https://doi.org/10.1016/j.geoderma.2012.02.005

Pinto, A. S., Bustamante, M. M. C., Kisselle, K., Burke, R., Zepp, R., Viana, L. T., Varella, R. F., Molina, M. (2002). Soil emissions of N_2O, NO, and CO_2 in Brazilian Savannas: Effects of vegetation type, seasonality, and prescribed fires. *Journal of Geophysical Research*, *107*, 1–9. https://doi.org/10.1029/2001jd000342

Rey, A., Oyonarte, C., Morán-López, T., Raimundo, J., Pegoraro, E. (2017). Changes in soil moisture predict soil carbon losses upon rewetting in a perennial semiarid steppe in SE Spain. *Geoderma*, *287*, 135–146. https://doi.org/10.1016/j.geoderma.2016.06.025

Robinson, D. A., Hopmans, J. W., Filipovic, V., van der Ploeg, M., Lebron, I., Jones, S. B., Reinsch, S., Jarvis, N., Tuller, M. (2019). Global environmental changes impact soil hydraulic functions through biophysical feedbacks. *Global Change Biology*, *25*, 1895–1904. https://doi.org/10.1111/gcb.14626

Schimel, J. P. (2018). Life in Dry Soils: Effects of Drought on Soil Microbial Communities and Processes. *Annual Review of Ecology, Evolution, and Systematics*, *49*, 409–432. https://doi.org/10.1146/annurev-ecolsys-110617-062614

Schymanski, S., Grahm, L., Or, D. (2017). The physical origins of rapid soil CO_2 release following wetting. Presented at the EGU General Assembly 23-28 April 2017, Vienna.

Serrano-Ortiz, P., Roland, M., Sanchez-Moral, S., Janssens, I. A., Domingo, F., Goddéris, Y., Kowalski, A. S. (2010). Hidden, abiotic CO_2 flows and gaseous reservoirs in the terrestrial carbon cycle: Review and perspectives. *Agricultural and Forest Meteorology*, *150*, 321–329.

https://doi.org/10.1016/j.agrformet.2010.01.002

Shakesby, R. A., Doerr, S. H. (2006). Wildfire as a hydrological and geomorphological agent. *Earth-Science Reviews*, *74*, 269–307. https://doi.org/10.1016/j.earscirev.2005.10.006

Smith, A. P., Bond-Lamberty, B., Benscoter, B. W., Tfaily, M. M., Hinkle, C. R., Liu, C., Bailey, V. L. (2017). Shifts in pore connectivity from precipitation versus groundwater rewetting increases soil carbon loss after drought. *Nature Communications*, *8*, 1–11. https://doi.org/10.1038/s41467-017-01320-x

Sponseller, R. A. (2007). Precipitation pulses and soil CO_2 flux in a Sonoran Desert ecosystem. *Global Change Biology*, *13*, 426–436. https://doi.org/10.1111/j.1365-2486.2006.01307.x

Trenberth, K. E., Dai, A., van der Schrier, G., Jones, P. D., Barichivich, J., Briffa, K. R., Sheffield, J. (2013). Global warming and changes in drought. *Nature Climate Change*, *4*, 17. https://doi.org/https://doi.org/10.1038/nclimate2067

Urbanek, E., Shakesby, R. A. (2009). Impact of stone content on water movement in water-repellent sand. *European Journal of Soil Science*, *60*, 412–419. https://doi.org/10.1111/j.1365-2389.2009.01128.x

Urbanek, E., Walsh, R. P. D., Shakesby, R. A. (2015). Patterns of soil water repellency change with wetting and drying: The influence of cracks, roots and drainage conditions. *Hydrological Processes*, *29*, 2799–2813. https://doi.org/10.1002/hyp.10404

Urbanek, E., Doerr, S. H. (2017). CO_2 efflux from soils with seasonal water repellency. *Biogeosciences*, *14*, 4781–4794. https://doi.org/https://doi.org/10.5194/bg-14-4781-2017

van Reeuwijk, L. P. (2002). *Procedures for soil analysis* (Sixth). Wageningen: ISRIC, FAO.

Vargas, R., Collins, S. L., Thomey, M. L., Johson, J. E., Brown, R. F., Natvig, D. O, Friggens, M. T. (2012). Precipitation variability and fire influence the temporal dynamics of soil CO_2 efflux in

an arid grassland. *Global Change Biology*, *18*, 1401–1411. https://doi.org/10.1111/j.1365-2486.2011.02628.x

Vicca, S., Bahn, M., Estiarte, M., Van Loon, E. E., Vargas, R., Alberti, G., Ambus, P., Arain, M. A., Beier, C., Bentley, L. P., Borken, W., Buchmann, N., Collins, S. L., De Dato, G., Dukes, J. S., Escolar, C., Fay, P., Guidolotti, G., Hanson, P. J., Kahmen, A., Kröel-Dulay, G., Ladreiter-Knauss, T., Larsen, K. S., Lellei-Kovacs, E., Lebrija-Trejos, E., Maestre, F. T., Marhan, S., Marshall, M., Meir, P., Miao, Y., Muhr, J., Niklaus, P. A., Ogaya, R., Peñuelas, J., Poll, C., Rustad, L. E., Savage, K., Schindlbacher, A., Schmidt, I. K., Smith, A. R., Sotta, E. D., Suseela, V., Tietema, A., Van Gestel, N., Van Straaten, O., Wan, S., Weber, U., Janssens, I. A. (2014). Can current moisture responses predict soil CO_2 efflux under altered precipitation regimes? A synthesis of manipulation experiments. *Biogeosciences*, *11*, 2991–3013. https://doi.org/10.5194/bg-11-2991-2014

Wang, Q., He, N., Liu, Y., Li, M., Xu, L. (2016). Strong pulse effects of precipitation events on soil microbial respiration in temperate forests. *Geoderma*, *275*, 67–73. https://doi.org/10.1016/j.geoderma.2016.04.016

Waring, B. G., Powers, J. S. (2016). Unraveling the mechanisms underlying pulse dynamics of soil respiration in tropical dry forests. *Environmental Research Letters*, *11*. https://doi.org/10.1088/1748-9326/11/10/105005

729

Fig. 1. Example of representative intact core soil surfaces of the two experimental soils before wetting. BwA (left), BnoA (right).

730

731

732

733

734

735

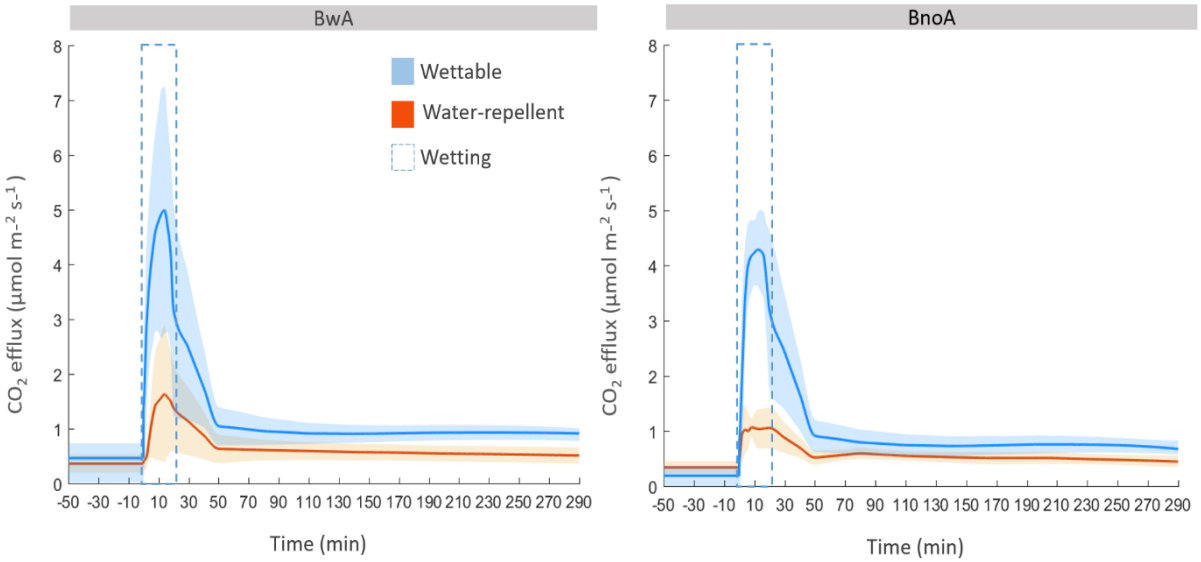

Fig. 2. Response of CO_2 efflux to wetting, with water (water-repellent scenario) and water mixed with wetting agent (wettable scenario), under laboratory conditions of recently burned soils with ash (BwA) and with ash removed (BnoA). The orange line and shaded area represent the mean response (n = 5) with 95% confidence interval to wetting under the water-repellent scenario and the blue line with shaded area represents the mean response (n = 5) with 95 % confidence intervals to wetting under the wettable scenario.

736

737

738

739

740

741

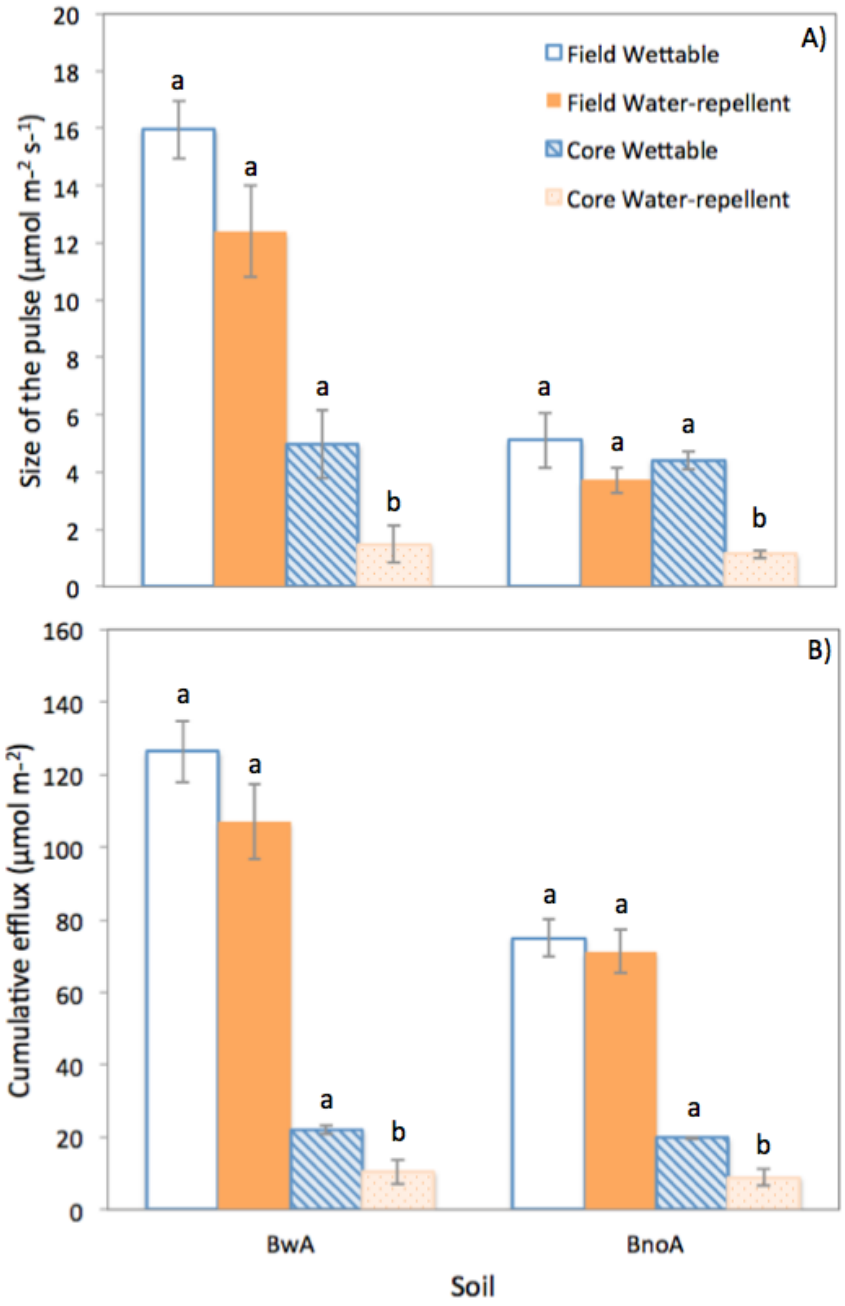

742 Fig. 3. **A)** Size of the CO_2 pulse and **B)** cumulative efflux after wetting under both field and core-
743 scale in burnt soils with ash (BwA) and ash removed (BnoA) under water-repellent (wetted with
744 water) and wettable (wetted with water and wetting agent) conditions. Values represent the
745 mean (n = 4 for field results, n = 5 for core results) with standard error bars. Different lowercase
746 letters (a-b) within the same site and scale (field vs. core-scale) indicate significant differences
747 between wettable and water-repellent conditions at $p < 0.05$.

748

749

750

751

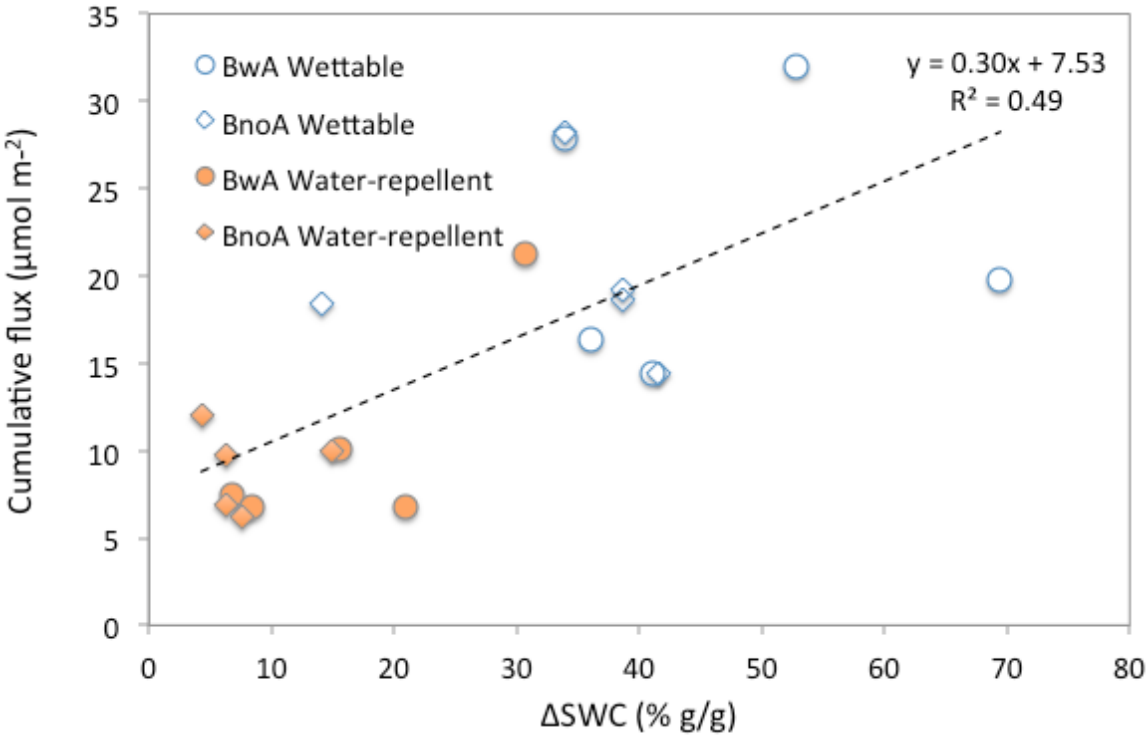

Fig. 4. Relationship between cumulative flux and the change in SWC with wetting under laboratory conditions (n = 5).

752

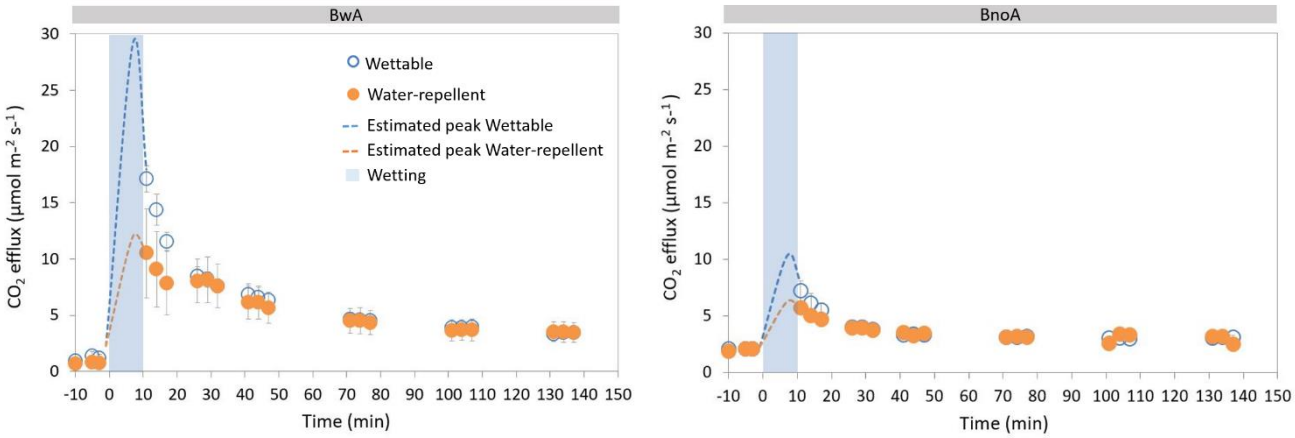

Fig. 5. CO_2 efflux response to wetting under field conditions for burnt soils with ash (BwA) and with ash removed (BnoA). Water-repellent scenario (orange shaded circles) represents wetting with water and wettable scenario (blue open circles) represent wetting with water and wetting agent. Missing CO_2 peaks under wettable and under water-repellent conditions are represented by the blue and orange dashed lines respectively. Values are the mean flux (n = 4) with 95 % CI.

753

754

755

756

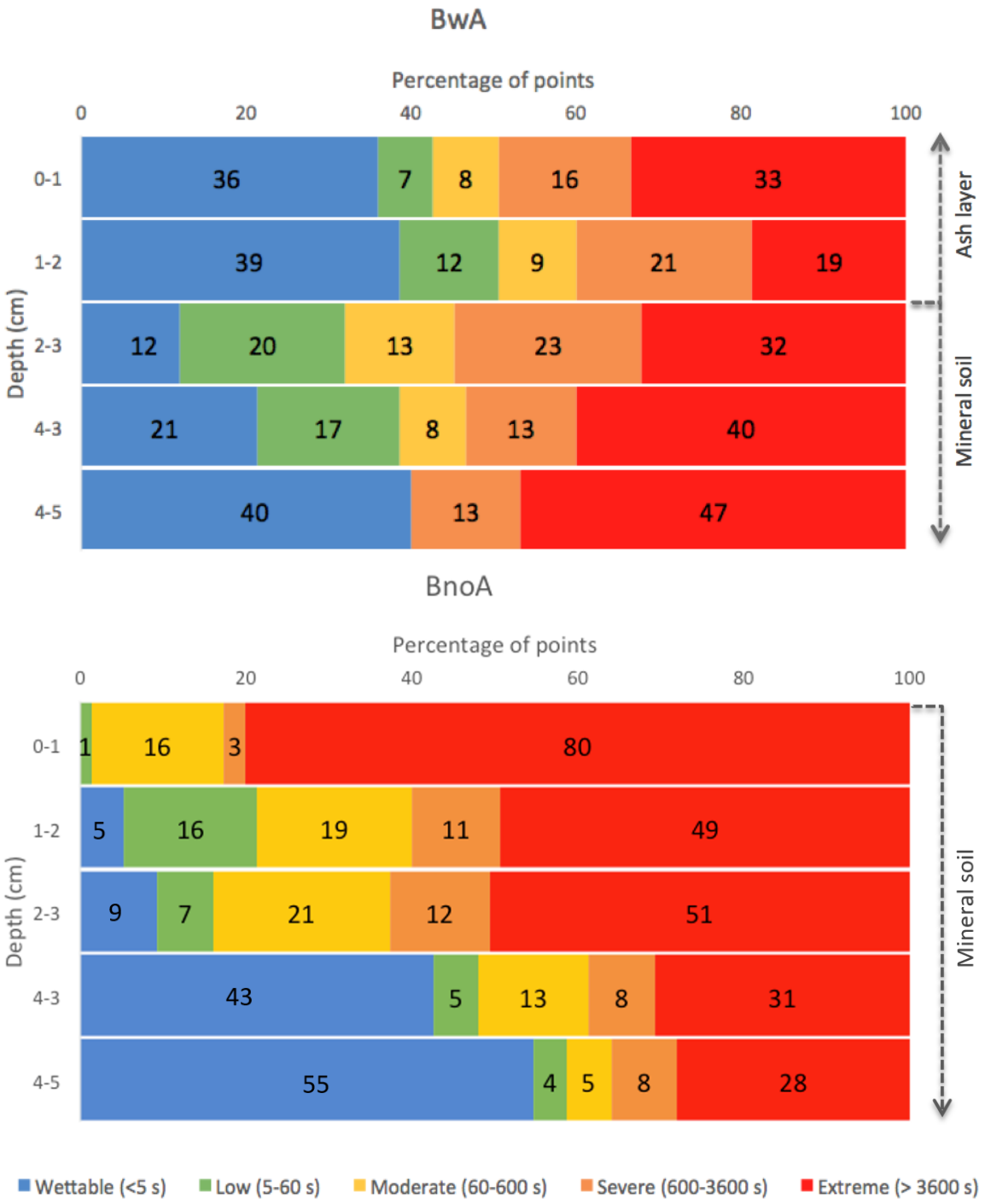

Fig. 6. Frequency distribution of SWR represented as the percentage of points for each repellency class in recently burned soils with ash layer (BwA) and ash layer removed (BnoA) (n = 75 per soil depth: 15 points per each core's depth × 5 cores per soil).

757

758

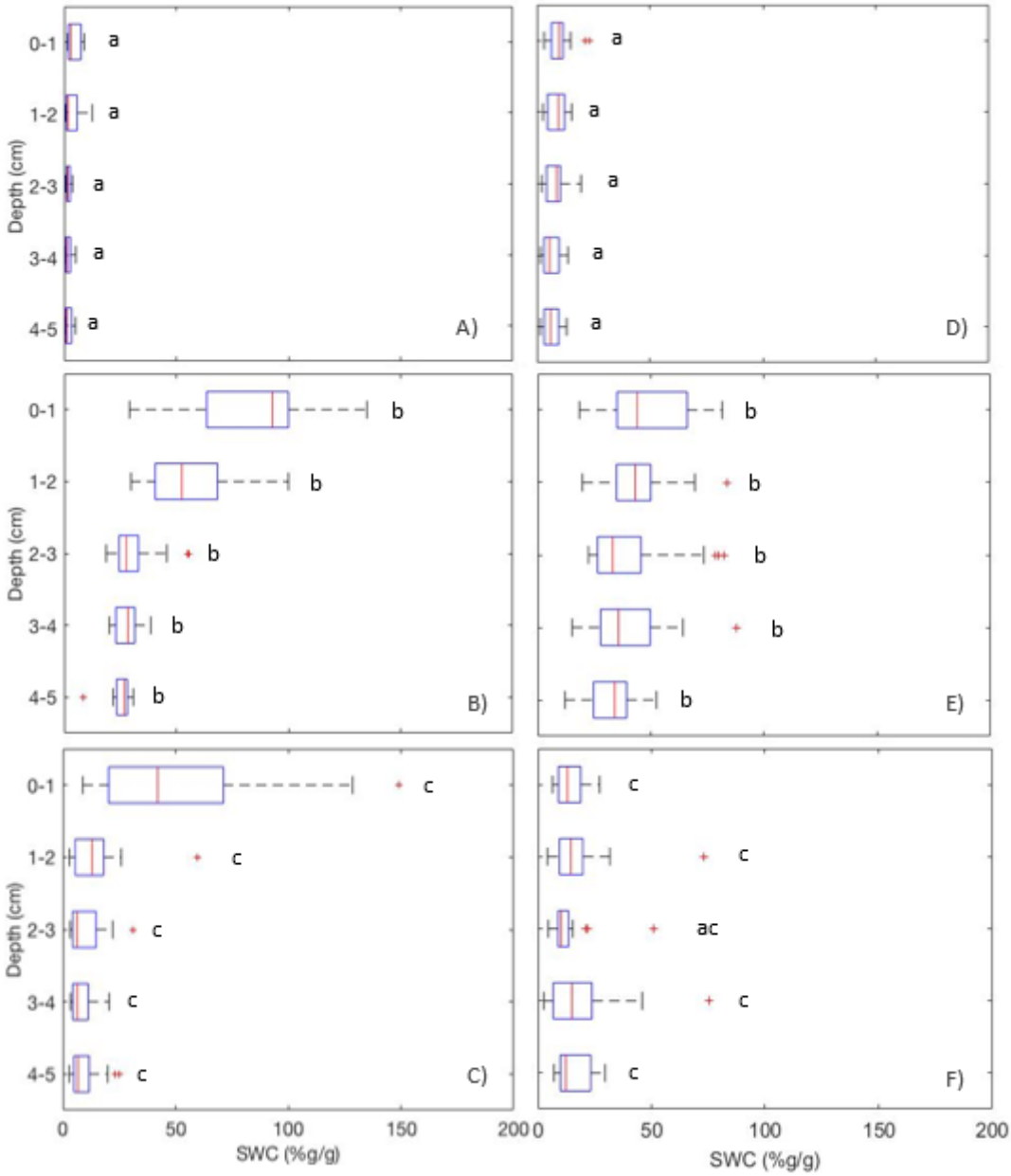

759 Fig. 7. SWC after wetting with depth. **A)** Burnt soil with ash (BwA) before wetting, **B)** BwA under
760 wettable scenario, **C)** BwA under water-repellent scenario, **D)** Burnt soil with ash removed
761 (BnoA) before wetting, **E)** BnoA under wettable scenario, **F)** BnoA under water-repellent
762 scenario. Central mark indicates the median, bottom and top edges indicate 25th and 75th percentiles. Whiskers represent maximum and minimum data points. Outliers are plotted as '+' and represent points that are 1.5 times less or greater than the 25^{th} and 75^{th} percentiles respectively. Different lowercase letters (a-c) within the same layer and site indicate significant differences between wettable and water-repellent conditions at a $p < 0.05$.

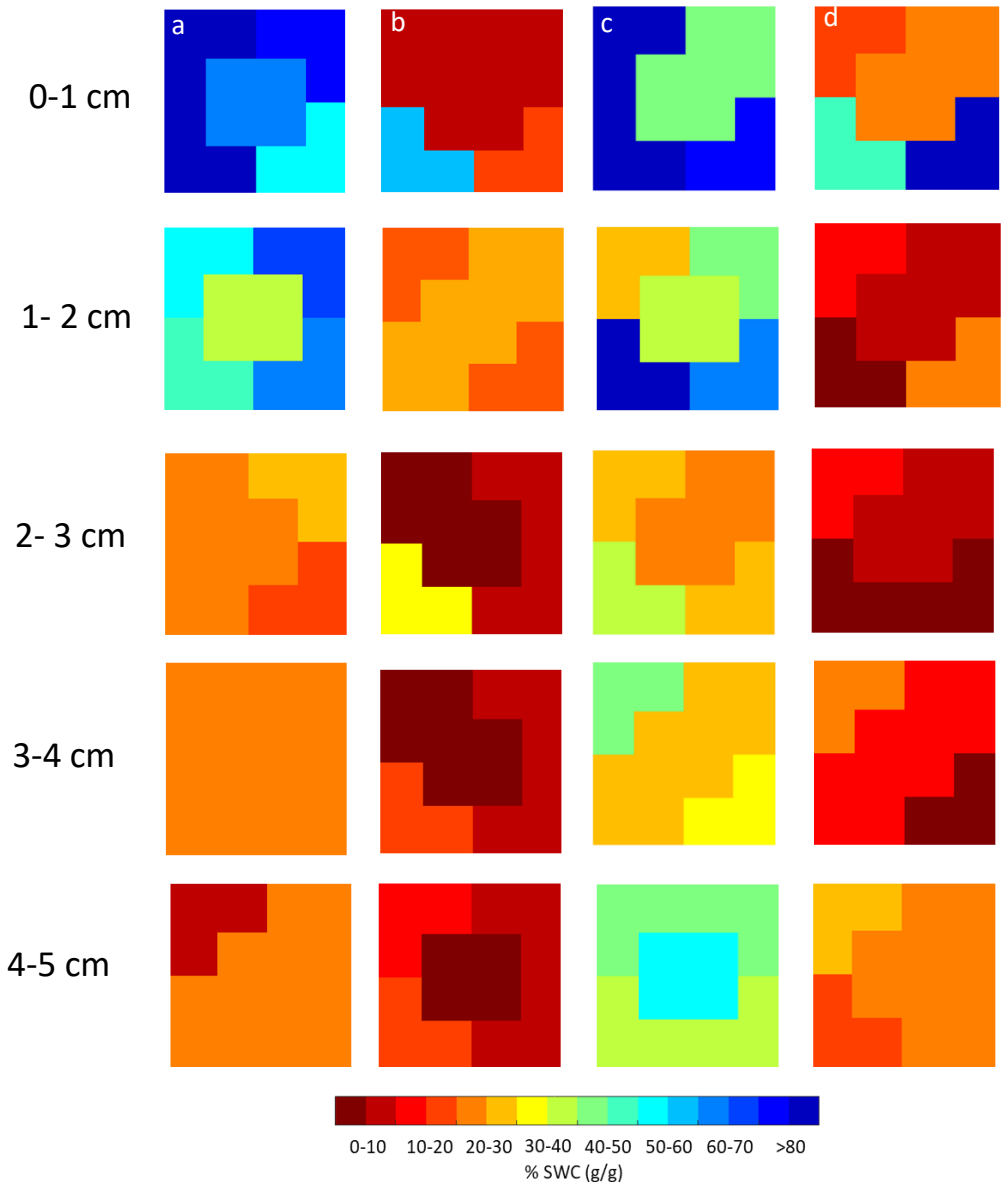

Fig. 8. Representative example of SWC distribution after wetting of intact core samples under laboratory conditions: a) Burnt soil with ash (BwA) under wettable conditions (wetted with water and wetting agent), b) BwA under water-repellent conditions (wetted with water), c) Burnt soil with ash removed (BnoA) under wettable conditions (wetted with water and wetting agent), d) BnoA under water-repellent conditions (wetted with water).

763

764

765 Table 1. General characteristics of the topsoil (0-5 cm depth) at the two recently burned soils with
766 ash (BwA) and with ash removed (BnoA). Values are the mean with SD in brackets. The ash layer
767 in the top 0 – 2 cm of the BwA soil was left untouched for all characterisation analysis.

	BwA	BnoA
Bulk density (n=10)	1.13 (0.11)	1.01 (0.11)
Stone content (% of total weight)	10.70 (3.85)	23.34 (8.57)
Texture (n=10)	Sandy loam	Sandy loam
% Sand	58.45 (7.49)	55.96 (5.21)
% Silt	36.28 (6.77)	37.50 (3.83)
% Clay	5.23 (1.27)	6.54 (1.55)
% Soil organic matter (SOM) with depth (< 2 mm fraction) (n=20)		
Overall % SOM (0 -5 cm)	8.50 (8.28)	11.34 (7.49)
0 - 1 cm	23.35 (9.30)	19.45 (1.30)
1 - 2 cm	10.35 (3.60)	15.44 (0.97)
2- 3 cm	4.85 (1.79)	8.53 (1.36)
3 - 4 cm	4.03 (1.33)	9.75 (1.05)
4 - 5 cm	3.99 (1.61)	7.88 (0.51)
% Soil water content (at time of sampling)	2.76 (2.22)	7.63 (3.75)
Surface water drop penetration test (s) (n=5)	2404 (3162)	9509 (5843)
Surface water repellency classification*	Strongly repellent	Extremely repellent

* According to Doerr (1998).

768

769

770

771

772 Table 2. Average SWC (measured volumetrically (% v v^{-1}) in the field and gravimetrically (% g g^{-1})
773 in the intact cores) before and after wetting with water (water-repellent scenario) and wetting
774 with water and wetting agent (wettable scenario). Values are the mean with SD.

		Water-repellent scenario					Wettable				
	Soil	Before wetting		After wetting		ΔSWC (%)	Before wetting		After wetting		ΔSWC (%)
Intact cores	BwA	2.8	(2.2)	19.3	(22.2)	**16.5**	2.8	(2.2)	49.4	(35.5)	**46.7**
(n = 10)	BnoA	7.6	(3.8)	15.5	(8.0)	**7.9**	7.6	(3.8)	41.0	(14.7)	**33.4**
In situ (n = 8)	BwA	1.6	(0.5)	15.8	(2.6)	**14.3**	1.9	(1.7)	18.5	(5.8)	**16.6**
	BnoA	4.4	(2.5)	20.3	(11.9)	**15.9**	4.2	(1.6)	26.7	(5.5)	**22.5**

775

776

777

778

779 Table 3. Time to drainage (min after the start of wetting) and drainage as a percentage of total
780 water added under laboratory conditions in burnt soils with ash (BwA) and ash removed (BnoA)
781 under water-repellent (wetted with water) and wettable (wetted with water and wetting agent)
782 conditions. Values are the mean with SD.

	Time to drainage (min)		Drainage (%)	
Soil	Water-repellent	Wettable	Water-repellent	Wettable
BwA (n =5)	3.4 (1.3)	12.3 (3.3)	76.3 (19.1)	14.0 (7.5)
BnoA (n = 5)	3.5 (1.9)	8.8 (6.1)	82.8 (12.6)	36.6 (29.0)

783

784

785